

Use of GIS and 3D visualisation to investigate radon problem in groundwater

Urška Demšar¹ and Kirlna Skeppström²

¹ Institute of Infrastructure,
Royal Institute of Technology (KTH), Stockholm, Sweden
urska.demsar@geomatics.kth.se

² Department of Land and Water Resources Engineering,
Royal Institute of Technology (KTH), Stockholm, Sweden
kirlna@kth.se

Abstract. Radon is radioactive and its origin in groundwater is principally linked to the content of its parent element, uranium or radium in bedrocks. However, an on-going research at the Department of Land and Water Resources Engineering shows that a number of factors other than bedrock may potentially influence the radon concentration in groundwater. These factors include: steepness of the terrain, soil type, distribution of uranium and the effect of fracture zone. This article presents an application of GIS and 3D visualisation to explore the radon problem in groundwater. After a GIS pre-processing, 3D visualisations of the thematic data were produced in order to see if the visual approach would be useful to preliminarily identify possible relationships between the high concentration of radon and other parameters.

1 Introduction

Geographical Information Systems (GIS) are increasingly being used to understand and analyse a wide range of environmental problems. This article presents an application of GIS and visualisation in the analysis of the radon problem in groundwater. The transformations and analysis of data to derive information or just for visualisation purposes are the most common applications of GIS [1, 2].

Visualisation is the graphical communication of information. When exploring data, humans look for structures, patterns and relationships between data elements. Such analysis is easier if the data are presented in a visual setting than in a textual or a numerical form. A visualisation provides an overview of complex and large datasets, shows a summary of data and helps in the identification of possible patterns and structures in the data [6]. The graphical representation should be simple enough to be easily understood, but complete enough to reveal all information present in the model. A 3D representation in a 2D display projects three locational dimensions onto a 2D plane. Using a set of perceptual depth cues to reinforce this projection, such as perspective, occlusion and parallax motion, a new cartographic degree of freedom is added to the visual representation. This can be done because of the characteristics of the human

perception to reconstruct genuinely 3D scenes from 2D retinal projections. Because of this, a 3D visualisation helps the viewer to easily gain knowledge of the relative layout and distances between objects [6, 24, 26].

There are many methods of representing complex geographical and geological data in 3D. Some of the more common ones used in geology and geosciences include layering [20], fence diagrams [20], solid models [9], wire-frame models [9] and 3D surfaces [20]. A general approach to produce a 3D surface from geographical information is to map the two basic geographical dimensions, longitude and latitude, to the x and y-axis respectively and show the variable of interest on the z-axis. Over this surface some other type of geographical information can be draped to provide texture: a thematic map or a satellite image [16]. Traditionally in geosciences the attribute mapped to the z-axis represents the third dimension in the real world, the elevation above the sea level (a digital elevation model) or the depth of the sea bottom. Examples include a 3D surface representing the bottom of the Baltic sea with added hydrological and environmental data [17] and satellite images and geomorphologic data draped over a DEM [23]. In some cases, the attribute mapped to the z-axis represents time. This kind of visualisation is not often encountered in geosciences, but is very common in time-geography [15] and in transportation studies [18]. The third type of 3D surface is the abstract surface, where the z-axis attribute represents neither a real geographic dimension nor time, but some other variable of interest. For example, the z-axis can represent the population density, the temperature [26], the density of human activity or travel [18], the river/stream flow [5], or, in geosciences, the magnetic variation [11] or the kriging variance [3].

The 3D surface can be displayed in several ways, either as an isoline map [1], drawn as a perspective image in so-called 2.5D display [1] or as an interactive 3D model which gives the possibility of interactive navigation, either in a 3D GIS environment or using VRML [16].

Prior to constructing a 3D visualisation and performing any analysis within a GIS, accurate raster surfaces need to be produced or acquired [19]. Very often, phenomena under investigation are characterised by scattered point data and interpolation or approximation methods are necessary to predict values at unsampled locations [1, 2]. For interpolation of the data in this study the following two methods were considered: Inverse Distance Weighted interpolation (IDW) and kriging (geostatistical approach). The former is based on the assumption that the value at an unsampled point can be approximated as a weighted average of values at points within a certain cut-off distance, or from a given number of the closest points [19]. Kriging is based on a concept of random functions: the surface or volume is assumed to be one realisation of a random function with a certain spatial covariance [2]. Kriging also forms weights from surrounding measured values to predict values at unmeasured locations as with IDW interpolation, but kriging weights come from a semivariogram that was developed by looking at the spatial structure of the data [3, 12]. In simple mathematical formula, kriging can be described as

$$Z(s) = \mu(s) + \varepsilon(s),$$

where $Z(s)$ represents the investigated phenomena, $\mu(s)$ deterministic trend and $\varepsilon(s)$ a random autocorrelated error. Different types of kriging are based on modified versions of the above formula [2].

The present study focuses on the problem of radon in groundwater. Radon is radioactive and its origin in groundwater is principally linked to the content of its parent element, uranium or radium in bedrocks [13, 25, 28]. Among the different rock types that exist, granites are most problematic since they contain increased concentrations of uranium [10]. Previous studies involving the use of GIS to investigate the radon problem are few and have mainly been focused on radon as an indoor hazard [8, 14, 27]. In [21] GIS and geostatistical analyses were used to study the spatial correlation between radon in groundwater and bedrock uranium. The hypothesis of an ongoing research project [22] states that a number of other factors (natural as well as technical) may be accountable for an increased radon concentration in groundwater. These factors include: bedrock, soil type, slope of a terrain, the occurrence and distribution of uranium in soils and the effect of fracture zone near a well.

This article presents an application of a 3D surface visualisation of geological and other thematic data related to the radon problem. The objective is to investigate if a relationship between high radon concentration and other factors can immediately be deduced through visualisation. A 3D surface visualisation was chosen as a potentially useful way to see if there are any obvious spatial connections between high radon values and different thematic data. The interest was in detecting a relationship between two variables that are both locationally dependent. In a traditional 2D map, these two variables would both be represented by graphical symbology, but in a 3D visualisation, one variable can be represented as the new degree of freedom and the other one with graphical symbology of the draped thematic map. The relationship between the two variables can therefore be detected by comparing the location of the graphical clues of the second variable to the relative position of the characteristics features (peaks or valleys) on the surface produced by the first variable.

2 Study area

The study area was located in the central part of Stockholm County (fig. 1). The spatial extent ranged from 6599975 to 6625025 in the north direction and from 1624975 to 1650025 in the east direction, i.e. an area of approximately 25 x 25 km. A total of 293 drilled wells located in the study area have been subject to investigation.

3 Data and methodology

Thematic maps of soil, bedrock, elevation, fracture distribution as well as uranium occurrence were used for visualisation (table 1). Data were provided by the Swedish Geological Survey (SGU) and the Swedish National Land Survey. Radon concentrations for private wells were provided by municipalities. Data

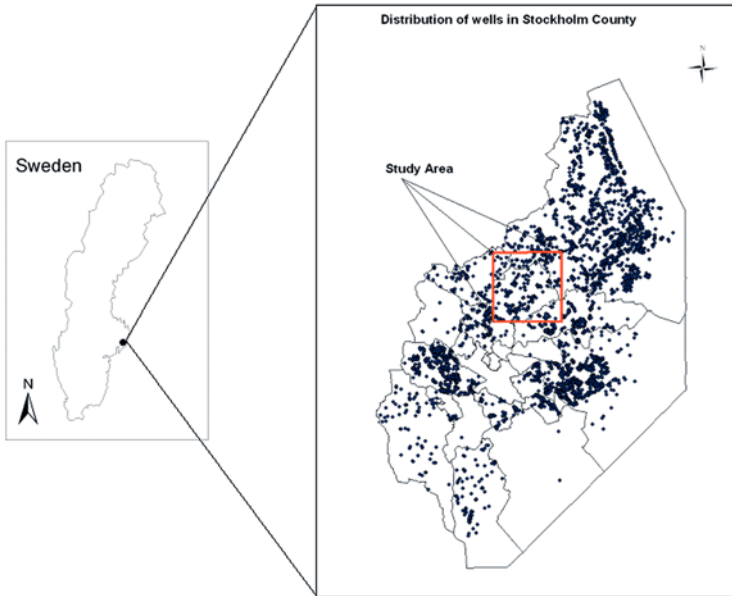


Fig. 1. Study area in Stockholm County.

were obtained in various formats, but most of them were converted into raster format with 50m spatial resolution for the purpose of visualisation.

Table 1. Data used for visualisation

Thematic map	Original format
elevation	raster file
soil	shape file - polygon
fracture distribution	shape file - line
bedrock	shape file - polygon
relative altitude within 200m	raster file (derived from elevation)
slope	raster file (derived from elevation)
uranium	ASCII file
radon concentrations	ASCII xyz

Radon data were obtained from municipalities. Samples were collected by either health officers or property owners and were sent to laboratories for analysis. No information about sampling techniques or measurement accuracy is available and thus the authors of this paper are in no position to discuss the various uncertainties involved. By visual inspection, the samples are considered to be well spread in the study area but data distribution is positively skewed with about 15

points considered to be outliers (exceeding 2000 Bq/l). The outliers were however not excluded in the analysis since high radon values can actually occur in reality and were instead considered to be an interesting case study.

For the transformation, analysis and visualisation of the data, the ArcGIS software was used. Soil maps and bedrock obtained as shape files, were rasterized with a spatial resolution of 50m to produce continuous surface maps. In order to estimate the steepness of the terrain, the slope data was derived from the elevation data. The relative altitude within 200 m was also derived from elevation data to provide an alternative indication of the steepness of the terrain as expressed in the following formula:

$$RA(x) = \frac{E(x) - E_{min}(x)}{E_{max}(x) - E_{min}(x)} \cdot 100,$$

where RA is relative altitude in %, $E(x)$ elevation of the current location x (pixel), $E_{min}(x)$ minimum elevation within 200 m and $E_{max}(x)$ maximum elevation within 200 m from the current location.

Radiometric data for uranium concentration were transformed from a series of point measurements along lines and interpolated using inverse distance weighting to produce a surface map. The radon concentration data were transformed into a point shape file and further interpolated by inverse distance weighting (IDW) resulting to a radon surface, which served as the basis for all visualisations. The interpolation methods IDW and kriging were compared in terms of their interpolation power and it was observed that surfaces created by IDW method are more accurate and better preserve the main patterns of variation. Similar observations have been made in [21].

A 3D visualisation of radon surface was produced using the 3D part of the ArcGIS software, ArcScene. In the resulting model, the x and y axes represented the two geographical directions (east and north respectively), while the z axis showed the radon concentration values. The 3D visualisation of radon surface, with indicated locations of wells is shown in fig. 2.

This radon surface was used as a base 3D structure for all other visualisations. All other thematic maps were in turn draped over this surface in order to produce a 3D model, which might reveal a potential relationship between the radon values and the mapped attribute. These visualisations and the conclusions drawn from each of them are described in the following section.

4 Results

The visualisations in this section show the 3D radon surface with the maps of elevation, soil, bedrock, fracture lines, uranium content, slope and relative elevation draped over it.

4.1 Relationship between radon and elevation

As can be deduced from fig. 3, the wells with high radon values seem to be situated on low elevations and wells with lower radon values on higher elevations.

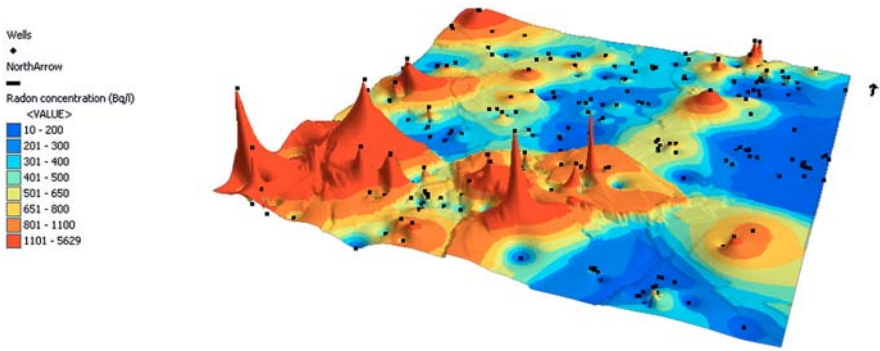


Fig. 2. A 3D visualisation of the surface, interpolated from the radon concentration measurements. The black dots on the surface mark the position of the wells.

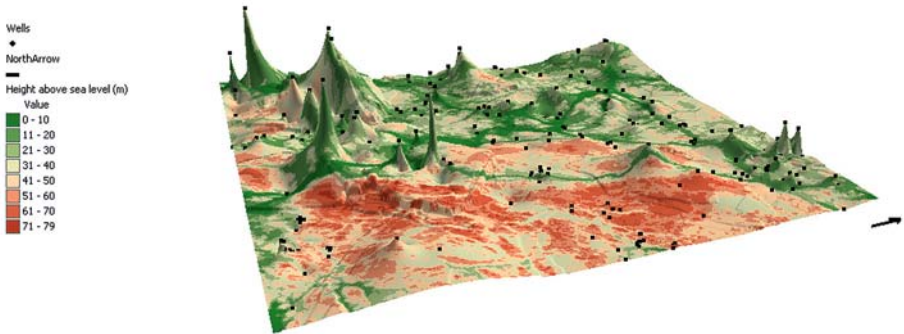


Fig. 3. A raster map of elevation draped over the interpolated radon surface. The height above sea level is represented using the colours on the map.

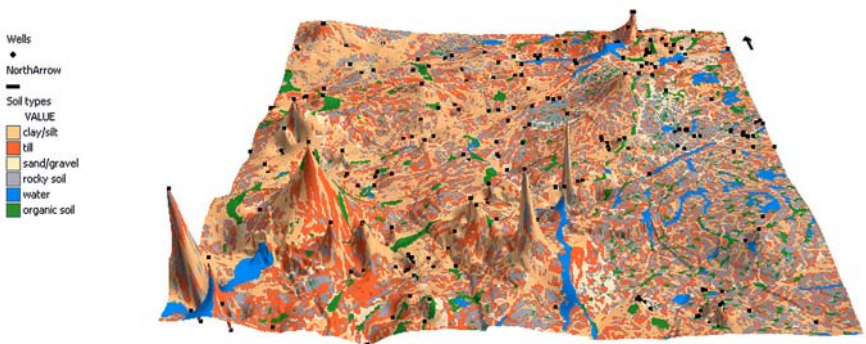


Fig. 4. A map of soil type draped over the radon surface.

4.2 Relationship between radon and soil types

From this visualisation (fig. 4) it can be deduced that higher values of radon correspond to areas with either till or clay. In the area studied, sand as overlying geology is lacking and thus no conclusion could be drawn with respect to sand.

4.3 Relationship between radon and bedrocks and relationship between radon and fracture lines

The next visualisation is an example of a multi-dimensional visualisation of five different variables. As in all visualisations, the three spatial dimensions represent the two-dimensional geographical extent and the radon concentrations. Additionally the fourth variable, indicated by the colour scheme, gives information on the bedrock type. The fifth variable is represented by draping the fracture lines data over the produced model, as shown in fig. 5.

The analysis of the visualisation of bedrock and fracture zones confirmed the expected geophysical relationship between the radon values and the type of bedrock. Wells with the highest radon values are situated upon granite and felsic gneisses. Some of the less extreme but still high concentrations are situated on the meta-sedimentary rocks.

A closer inspection of the visualisation also revealed some indications about the relationship between the radon concentrations and the locations of fracture lines. There seems to be a general trend that wells with high radon values also lie very near or on actual fracture lines, which are fractures (or faults or cracks) that exist naturally in bedrocks. Some peaks on the radon surface that indicate this trend are shown in fig. 6.

4.4 Relationship between radon and uranium

As the visualisation on the fig. 7 indicates, peaks of high radon concentrations are not necessarily located in regions where the content of uranium is the highest. On the contrary, the results are varied. Some peaks are encountered when the uranium content is exceeding 6 ppm and in other places, high radon concentrations are occurring when the uranium is less than 2 ppm

4.5 Relationship between radon and slope and relative elevation

Most of the peaks of high radon concentrations are not located on steep terrains as can be deduced from fig. 8. That conclusion is however not that obvious for the relative altitude within 200 m. In fig. 9, high radon concentrations can be observed at different levels of steepness.

5 Discussions and future work

3D visualisation has proved to be an interesting tool in analysing the various relationships that exist between radon concentration in water and other investigated

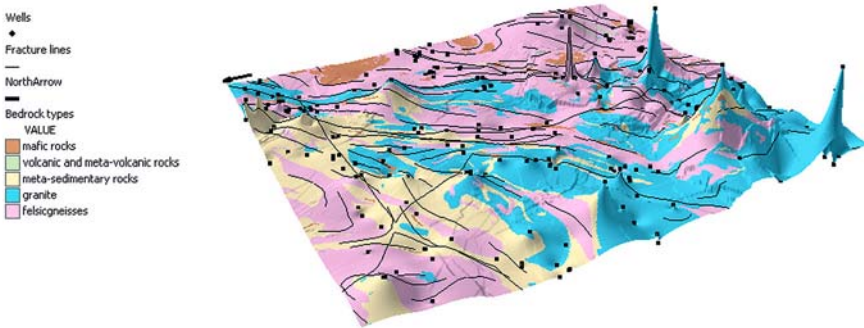


Fig. 5. A raster map of bedrock and a vector map of fracture lines draped over the interpolated radon surface.

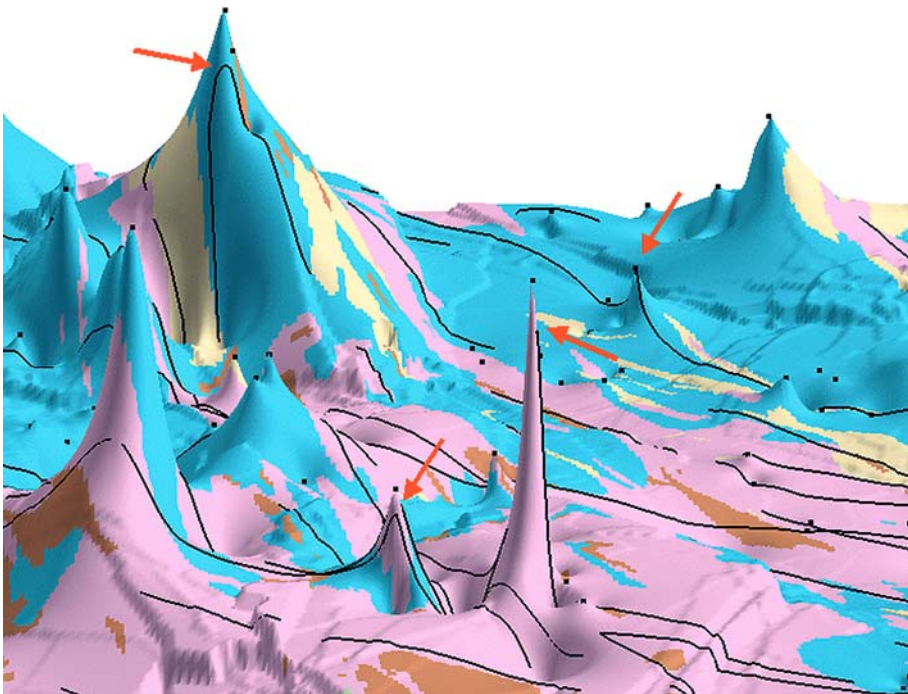


Fig. 6. A detailed view of the bedrock-fracture lines-radon visualisation. The red arrows indicate the peaks with high radon values that are situated near or on fracture lines.

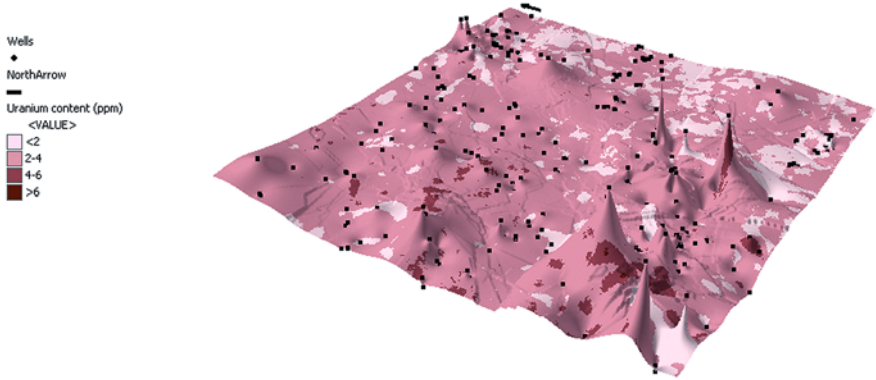


Fig. 7. The map of uranium content draped over the radon surface.

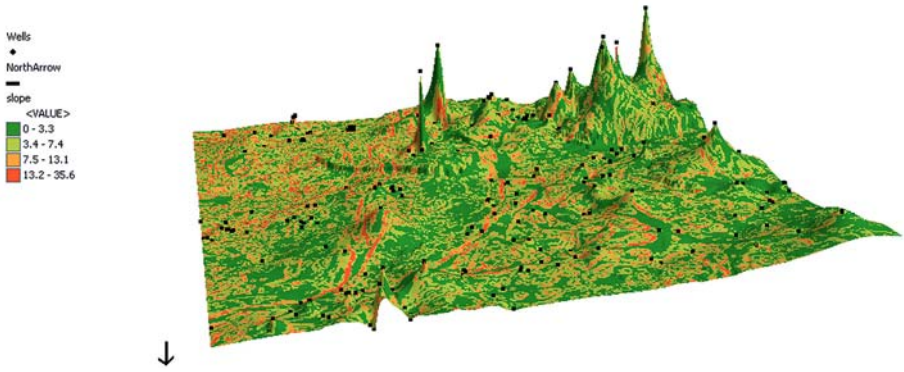


Fig. 8. A slope map (in %), derived from the elevation map, on the radon surface.

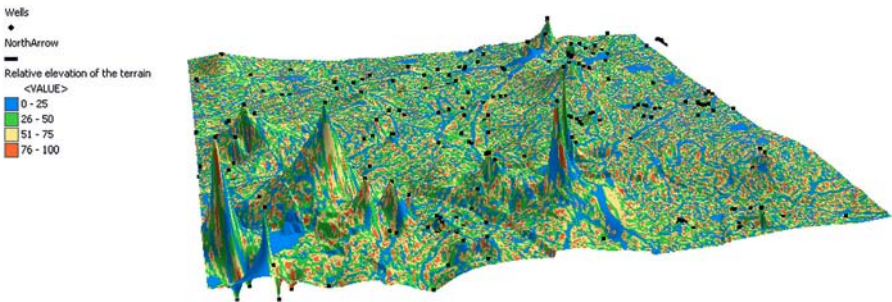


Fig. 9. A map of relative elevation within 200 m (in %) on the radon surface.

factors. The effects of peaks and depressions in a surface combined with colour effects provide an excellent medium for analysis purposes. The relationship between radon and granite rocks is clear and is as expected. Peaks of high radon concentrations were located on rocks that contain high uranium concentrations, the parent element of radon. However, the fact that high radon concentrations have also been registered in uranium poor areas points to the fact that some complex hydrological transport processes are probably accountable for high radon concentrations in those areas. The effect of slope influences the direction as well as the velocity of flow of groundwater. Water tends to flow rapidly from high altitude to low altitude so that sampled water in relatively flat terrains is expected to have higher radon concentrations. It has also been observed that peaks of high radon concentrations occur quite near to a fracture zone, where uranium enrichment is liable to occur.

There are however some limitations in using 3D visualisation for analysing the problem of radon in water. The effects of some factors are difficult to perceive through visualisations. Raster surfaces are not always possible to generate for some factors. In addition, it has also been observed that results of visualisations sometimes contradict established scientific facts. An interesting relationship detected in a visualisation might be coincidental, and a post-applied expert evaluation as well as a statistical evaluation are therefore crucial.

Table 2. Observed relationship between radon and investigated variables.

Variable	Observed relationship with radon	Detected by	
		statistics	visualisation
elevation	lower radon values occur on higher altitudes	yes	yes
soil type	higher radon values on clay/silt, lower radon values on sand/gravel, varied on till	yes	partially yes
bedrock	higher radon values on granites	yes	yes
distance to fracture lines	radon concentration decreases with distance from the fracture line	yes, but not statistically significant	yes
uranium	positive correlation between radon and uranium	yes	no, varied results
slope	not evident	no	relationship observed, but questionable
relative elevation	not evident	no	no, varied results

Results of visualisations were compared with statistical results performed in another study [22] and the comparisons are summarized in table 2. Some of the

relationships that were clearly detected by statistical analysis were also observed using the 3D visualisation. However one of the very strong relationships, between radon and uranium, was not evident from the visualisation. In one case, when observing slope, visualisation indicated a possible relationship, while statistical analysis did not result in any evident connection.

The ongoing PhD project at the Department of Land and Water Research Engineering has used the technique of multivariate analysis of data to investigate the factors in details. In addition, a risk modelling based on statistics has been performed and the output was used in GIS to generate prediction maps for areas at risk for high radon concentrations. Results of the study will be presented shortly [22].

Another way to detect the complex relationships between radon concentration and other environmental factors would be by using visual data mining. This process is based on the human ability to recognise unknown patterns and correlations from a visualisation of the data. The data is displayed in several different interconnected visualisations (graphs, charts, geographical visualisations, etc.). In the next step the human user recognizes a pattern, draws conclusions and interacts with the data. The visual system can also include automatic data mining algorithms for pre-processing the data before the visualisation, in order to structure the multidimensional data space and make the data easier to understand [4, 7]. Visual data mining could be applied to the data from the radon study and analysed in order to see if there exist any apparent multidimensional patterns. The results could be compared with the results of the risk modelling approach and the system should be tested by usability engineering. The aim of this analysis would be to see if visual data mining could be an adequate tool for geoscientists to use for approaching this type of environmental problem.

6 Acknowledgements

The authors gratefully acknowledge the support of Swedish Geological Survey (SGU) for financial support for the ongoing research of radon in groundwater at the Department of Land and Water Resources Engineering, KTH.

7 Contributors

Authors names are given in alphabetical order. Both authors are PhD students at the Royal Institute of Technology in Stockholm. Urška Demšar is working in the field of geovisualisation. Kirlna Skeppströms research is dedicated to the radon problem in groundwater. They have written this paper as a joint contribution.

References

1. Bohnam-Carter G. F., *Geographic Information Systems for Geoscientists: Modeling with GIS*, Elsevier, UK, 1998.

2. Burrough P.A. and McDonnell R.A., *Principles of Geographical Information Systems*, Oxford University Press, United States, 2000.
3. Carr J. R., *Data Visualization in the Geological sciences*, Prentice Hall, Upper Saddle River, 2002.
4. Demšar U., *Exploring geographical metadata by automatic and visual data mining*, licenciate thesis, KTH, Stockholm, 2004.
5. Drogue G., Pfister L., Leviandier T., Humbert J., Hoffmann L., El Idrissi A. and Iffly J. F., Using 3D dynamic cartography and hydrological modelling for linear streamflow mapping, *Computers & Geosciences*, 28:981-994, 2002.
6. Fayyad U., Grinstein G. G. and Wierse A., *Information Visualization in Data Mining and Knowledge Discovery*, Morgan Kaufmann, San Francisco, 2002.
7. Gahegan M., Takatsuka M., Wheeler M. and Hardisty F., Introducing GeoVISTA Studio: an integrated suite of visualization and computational methods for exploration and knowledge construction in geography, *Computers, Environment and Urban Systems*, 26:267-292, 2002.
8. Geiger C. and Barnes K., Indoor radon hazard: a geographical assessment and case study, *Applied Geography*, 14:350-371, 1994.
9. Gong J., Cheng P. and Wang Y., Three-dimensional modeling and application in geological exploration engineering, *Computers & Geosciences*, 30:391-404, 2004.
10. Gundersen L.C.S. and Wanty R.B. (eds.), *Field Studies of Radon in Rocks, Soils, and Water*, United States Government Printing Office, Washington DC, 20402, 1991.
11. De Kemp E. A., 3-D visualization of structural field data: examples from the Archean Caopatina Formation, Abitibi greenstone belt, Quebec, Canada, *Computers & Geosciences*, 26:509-230, 2000.
12. Kitanidis P.K., *Introduction to Geostatistics: Applications to Hydrogeology*, Cambridge University Press, 1997.
13. Knutsson G. and Olofsson B., Radon content in groundwater from drilled wells in the Stockholm region of Sweden, *NGU-bulletin*, 79-85, 2002.
14. Kohli S., Sahlén K., Löfman O., Sivertun Å., Foldevi M., Trell E. and Wigertz O., Individuals living in areas with high background radon: a GIS method to identify populations at risk, *Computer Methods and Programs in Biomedicine*, 53:105-112, 1997.
15. Kraak M.-J. and Koussoulakou A., A Visualization Environment for the Space-Time Cube, in: Fisher P. F. (ed.), *Developments in Spatial Data Handling*, 11th International Symposium on Spatial Data Handling, 189-200, Springer Verlag, Berlin Heidelberg, 2004.
16. Kraak M.-J. and Ormeling F., *Cartography: Visualization of Geospatial Data*, 2nd edition, Prentice Hall, Harlow, England, 2003.
17. Kreuseler M., Visualization of geographically related multidimensional data in virtual 3D scenes, *Computers & Geosciences*, 26:101-108, 2000.
18. Kwan M. P., Interactive geovisualization of activity-travel patterns using three-dimensional geographical information systems: a methodological exploration with a large data set, *Transportation Research Part C*, 8:185-203, 2000.
19. Longley P. A., Goodchild M. F., Maguire D. J. and Rhind D. W., *Geographic Information Systems, Vol 1.: Principles and Technical Issues*, 2nd edition, John Wiley and sons, New York, 1999.
20. Raper J. (ed.), *Three dimensional applications in geographical information systems*, Taylor & Francis, London, 1989.

21. Salih M.I., Pettersson H.B.L., Sivertun Å. and Lund E., Spatial correlation between radon (^{222}Rn) in groundwater and bedrock uranium (^{238}U): GIS and geostatistical analyses, *Journal of Spatial hydrology*, 2(2):1-10, 2002.
22. Skeppström K., *Research in progress*, planned licenciate thesis, KTH, Stockholm, spring 2005.
23. Walsh S. J., Butler D. R., Malanson G. P., Crews-Meyer K. A., Messina J. P. and Xiao N., Mapping, modeling and visualization of the influences of geomorphic processes on the alpine treeline ecotone, Glacier National Park, MT, USA, *Geomorphology*, 53:129-145, 2003.
24. Ware C. and Plumlee M., 3D Geovisualization and the Structure of Visual Space, in: Dykes J., MacEachren A. M. and Kraak M.-J. (eds.), *Exploring Geovisualization*, 567-576, Elsevier, Oxford, 2005.
25. Wilkening M., *Radon in the environment*, Elsevier Science Publishers B.V., 1990.
26. Wood J., Kirschenbauer S., Döllner J., Lopes A. and Bodum L., Using 3D in Visualization, in: Dykes J., MacEachren A. M. and Kraak M.-J. (eds.), *Exploring Geovisualization*, 295-312, Elsevier, Oxford, 2005.
27. Zhu H.C., Charlet J.M. and Poffijn A., Radon risk mapping in southern Belgium: an application of geostatistical and GIS techniques, *The science of the Total Environment*, 272:203-210, 2001.
28. Åkerblom G. and Lindgren, J., Mapping of groundwater radon potential, *Environmental Geology*, 13-22, 1996.